

Heterogeneous Contrastive Learning: Encoding Spatial Information for Compact Visual Representations

Xinyue Huo^{1,2} Lingxi Xie² Xiaopeng Zhang² Longhui Wei^{1,2}
Hao Li³ Zijie Yang⁴ Wengang Zhou¹ Houqiang Li¹ Qi Tian²
¹University of Science and Technology of China, ²Huawei Inc.
³Shanghai Jiao Tong University, ⁴Chinese Academy of Sciences

xinyueh@mail.ustc.edu.cn {198808xc, zxphistory, wlh2568@gmail.com

lihao0374@sjtu.edu.cn yangzijie@ict.ac.cn {zhwg, lihq}@ustc.edu.cn tian.qil@huawei.com

Abstract

Contrastive learning has achieved great success in self-supervised visual representation learning, but existing approaches mostly ignored spatial information which is often crucial for visual representation. This paper presents **heterogeneous contrastive learning (HCL)**, an effective approach that adds spatial information to the encoding stage to alleviate the learning inconsistency between the contrastive objective and strong data augmentation operations. We demonstrate the effectiveness of HCL by showing that (i) it achieves higher accuracy in instance discrimination and (ii) it surpasses existing pre-training methods in a series of downstream tasks while shrinking the pre-training costs by half. More importantly, we show that our approach achieves higher efficiency in visual representations, and thus delivers a key message to inspire the future research of self-supervised visual representation learning.

1. Introduction

Deep learning [19] opens a new era for visual representation learning, yet most deep learning methods are built upon a large corpus of labeled data. Due to the high costs in data annotation, the community urges new algorithms that can make use of unlabeled data for learning representations, *e.g.*, effectively capturing data distribution in a high-dimensional space. Hence, self-supervised visual representation learning (S²VRL) has been an important topic [6, 10, 29] in recent years. In the early age, researchers have shown that deep networks, after pre-trained by some self-supervised tasks (*e.g.*, geometry prediction, colorization, *etc.*), often achieve faster convergence in downstream tasks (*e.g.*, object detection, semantic segmentation, *etc.*) as well as higher recognition accuracy.

Recently, the idea of contrastive learning [3, 2, 13, 17,

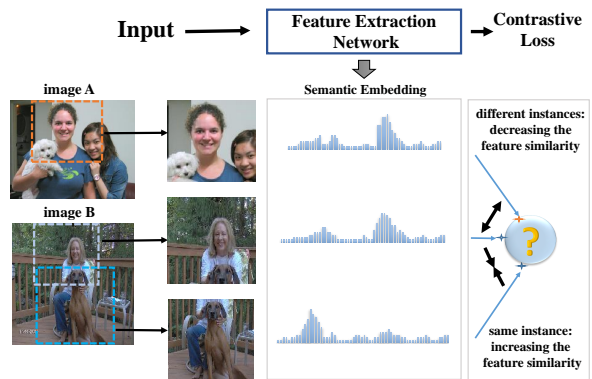


Figure 1. Existing contrastive learning methods assumed that all samples from the same image are closely embedded into the feature space. But, under strong data augmentation operations, the samples may have largely different semantics – sometimes, the sampled patch is closer to other images. This can confuse the learning process in finding compact visual representations.

[11] has largely boosted the performance of S²VRL. It works by encoding each image into a compact vector and asking the model to discriminate itself (often perturbed by data augmentation) from a large set of other instances. It is believed that to arrive at a high accuracy in instance discrimination, compact semantic information must be extracted, and thus the goal of representation learning is achieved [7]. To push the limit of semantic learning, researchers have also applied stronger data augmentation techniques and demonstrated the effectiveness in S²VRL [1, 21].

But, there is a critical issue that has been mostly neglected. Popular S²VRL methods such as SimCLR [2] and MoCo [13] do not encode spatial information in the representation vector, yet they require the vector to resist against some data augmentation operations (*e.g.*, image cropping and flipping) that are spatially sensitive. As shown in Figure 1, this implies that very close representation vectors are

assumed to be extracted from an image regardless of which region is cropped and whether it is flipped – in some extreme cases, the encoded vectors on some regions that have zero overlap on the original image are pulled towards each other by the contrastive objective, which can largely confuse the learning algorithm. In practice, this can downgrade the ability of pre-trained models when they are deployed to some downstream tasks that require spatial understanding, such as object detection and semantic segmentation.

Motivated by the above, we propose an effective approach named **heterogeneous contrastive learning** (HCL) that appends an individual branch to capture spatial information. In the encoding stage, HCL computes two feature vectors for semantic and spatial information, respectively. The semantic branch is identical to the existing approach that extracts a low-dimensional vector from the last average-pooled layer, followed by a multi-layer perceptron. The spatial branch, for sake of simplicity, follows the feature pyramid network [22], with the architecture slightly modified to fit the S²VRL task, to obtain another compact vector (often with a similar length) by integrating multi-stage visual features. These two vectors are then normalized and concatenated before fed into the contrastive loss function. Note that HCL only impacts the contrastive learning stage and the pre-trained model can be deployed to any downstream tasks with no further changes or costs.

We evaluate the effectiveness of HCL in a series of downstream tasks including object detection and semantic segmentation. HCL outperforms all existing S²VRL approaches in terms of recognition accuracy. In particular, compared to MoCo-v2 [3], HCL uses half of its pre-training costs but surpasses it by APs of 0.8% and 0.7% in MS-COCO object detection and instance segmentation, respectively, and the gain becomes more significant under higher IoU thresholds. We owe such improvement to a more efficient way of learning visual representations. To verify this, we use principal component analysis (PCA) to compress the learned features and perform offline contrastive testing. Under the same dimensionality (*e.g.*, 128-D), the mixed features (half semantic, half spatial) achieve higher accuracy in instance discrimination. This delivers a key message, possibly more important than the empirical results, that contrastive learning is indeed pursuing high **efficiency** and low **information loss** in visual representations, where the former partly reflects in the length of encoded features and the latter is measured by the instance discrimination error. From this viewpoint, HCL explained as heterogeneous features are more efficient visual representations, paving a new path for future research in S²VRL.

The rest of this paper is organized as follows. Section 2 briefly reviews related work, and Section 3 describes our approach. After experiments are shown in Section 4, we draw conclusions and deliver important messages in Section 5.

2. Related Work

Deep learning [19] has achieved great success in a wide range of computer vision problems. The core of deep learning is to build complicated functions named deep neural networks for learning visual representations. In the past years, the optimization of deep neural networks is largely relied on labeled data, for which the community built large-scale image datasets (*e.g.*, ImageNet [5], MS-COCO [23], *etc.*) to maximally cover real-world data distribution. However, there are two major drawbacks of the supervised learning paradigm: (i) the trained models often lack transferability to other domains, and (ii) the ability of exploring unlabeled data is weak. To alleviate these issues, researchers started to investigate unsupervised algorithms for learning visual representations.

This paper focuses on a subarea of unsupervised learning, named self-supervised visual representation learning (S²VRL). The goal is to capture the data distribution in an unlabeled dataset and (most often) store it in a deep neural network. Though the trained network does not make any semantic prediction, the initialized weights can assist the network training on labeled datasets, often referred to as the downstream tasks. The key of S²VRL is to find some image nature that corresponds to image semantics to some extent yet does not require any annotations. Typical examples include siamese networks learned from the consistency between the neighboring frames of videos [9, 39, 27, 20], predicting the spatial relationship between image patches [6] which later evolved into the jigsaw puzzle task [29, 40, 36, 31] predicting image-level information (*e.g.*, orientation [32], rotation [10, 26], counting [30], *etc.*), recovering image contents (*e.g.*, inpainting [33] and colorization [44, 18]), *etc.* These efforts achieved accuracy gain on downstream tasks over randomly initialized neural networks, but the performance is far behind the fully-supervised counterpart.

Recently, researchers have opened a new era by noticing that contrastive learning [13] is a promising pretext task for S²VRL. In contrastive learning, a low-dimensional feature vector is extracted from each image and the goal is to use the feature to identify the image among a gallery that contains a large number of images (*i.e.*, instance discrimination). In practice, the query image is often perturbed by some kind of data augmentation (*e.g.*, image cropping, flipping, *etc.*) and this is partly related to multi-view learning [38, 16]. To improve the performance, various modifications beyond the raw model have been proposed, including using a multi-layer perceptron to project the features to another space [2], building a large memory bank to increase the difficulty of instance discrimination [13], introducing stronger data augmentation operations to challenge the learning algorithm [37, 2], *etc.* With these upgrades, the S²VRL performance in downstream tasks is largely

boosted, even surpassing fully-supervised models due to the reduced extent in fitting the source task, *e.g.*, classification. There are also efforts in integrating supervision into contrastive learning [17], showing promising results in learning semantics, but the improvement does not seem consistent.

3. Our Approach

3.1. Preliminaries: Contrastive Learning

Self-supervised visual representation learning (S^2VRL) starts with an unlabeled image dataset, $\mathcal{S} = \{\mathbf{x}_n\}_{n=1}^N$, and aims to learn a mapping function, $\mathbf{y} = \mathbf{f}(\mathbf{x}) \doteq \mathbf{f}(\mathbf{x}; \boldsymbol{\theta})$, for compact feature representation. In the current era, $\mathbf{f}(\cdot)$ often appears as a deep network and $\boldsymbol{\theta}$ denotes the learnable parameters, *e.g.*, convolutional weights.

Contrastive learning is built upon the assumption that images sampled using different views from the same input image should be represented by similar features. Here, a sampling view indicates a set of operations (*e.g.*, image cropping and flipping) that slightly perturbs the input image. To quantify this request, for each training image, \mathbf{x} , two variants are sampled from it, *i.e.*, $\mathbf{x}_1 = \mathbf{s}(\mathbf{x}, \mathbf{v}_1)$ and $\mathbf{x}_2 = \mathbf{s}(\mathbf{x}, \mathbf{v}_2)$ where $\mathbf{s}(\cdot)$ is the sampling function and $\mathbf{v}_1, \mathbf{v}_2 \in \mathcal{V}$, the space of sampling views. To force the feature similarity between \mathbf{x}_1 and \mathbf{x}_2 , $\mathbf{f}(\mathbf{x}_1) \approx \mathbf{f}(\mathbf{x}_2)$, they are put into a gallery, \mathcal{G} , that contains a lot other images known as *distractors*, using \mathbf{x}_1 as the query, and requiring the network to discriminate \mathbf{x}_2 from other instances. This therefore becomes a classification problem and the corresponding loss function can be written as:

$$\mathcal{L}(\mathbf{x}_1, \mathbf{x}_2, \mathcal{G}) = -\log \frac{\text{sim}(\mathbf{x}_1, \mathbf{x}_2)}{\text{sim}(\mathbf{x}_1, \mathbf{x}_2) + \sum_{\mathbf{x}' \in \mathcal{G}} \text{sim}(\mathbf{x}_1, \mathbf{x}')}, \quad (1)$$

where $\text{sim}(\mathbf{x}_1, \mathbf{x}_2)$ is the similarity between \mathbf{x}_1 and \mathbf{x}_2 , often measured by computing the exponential inner-product between the corresponding embedded features and parameterized by the ‘temperature’ hyper-parameter, T :

$$\text{sim}(\mathbf{x}_1, \mathbf{x}_2) \equiv \exp\left\{\frac{1}{T} \cdot \mathbf{g}(\mathbf{x}_1)^\top \cdot \mathbf{g}(\mathbf{x}_2)\right\}, \quad (2)$$

where $\mathbf{g}(\mathbf{x})$ projects $\mathbf{f}(\mathbf{x})$ into a low-dimensional space for compacticity. This is often achieved by a multi-layer perceptron upon $\mathbf{f}(\cdot)$.

Recent advances [13, 2] has revealed several key points to improve the performance of contrastive learning, including using a sufficiently large gallery \mathcal{G} and adding data augmentation to enlarge the gap between \mathbf{x}_1 and \mathbf{x}_2 . Both the modifications can be explained as increasing the difficulty of instance discrimination, so that the algorithm is expected to learn a stronger representation function [1, 21].

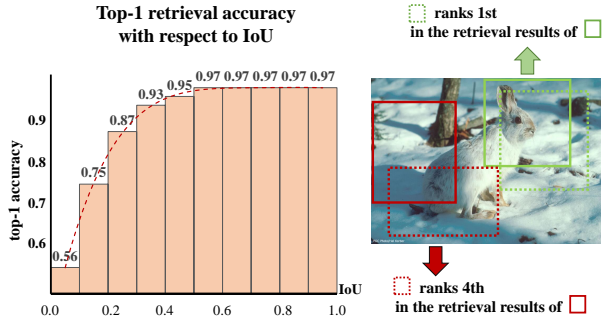


Figure 2. **Left:** the top-1 retrieval accuracy with respect to different correlation coefficients between the two samples. **Right:** a typical example showing that the retrieval accuracy is closely related to the correlation coefficient.

3.2. Inconsistency between Sampling and Learning

The above method has a significant drawback. On one hand, stronger data augmentations are verified effective to enhance the performance of contrastive learning. On the other hand, it becomes problematic to assume that two variants of an image to have close feature representations especially in the scenarios that they are irrelevant due to data augmentation. This is often a difficult task for the learning algorithm.

To verify this statement in statistics, we perform an offline *contrastive testing* to observe how the difference in sampling views affects instance discrimination. Details of contrastive testing are illustrated in Section 3.4. Briefly, we directly use a ResNet-50 model trained by MoCo-v2 [3] for 800 epochs on ImageNet-1K and traverse through the ImageNet-1K training set, checking whether the top-1 retrieved result is correct. Meanwhile, for each pair of images, \mathbf{x}_1 and \mathbf{x}_2 , we compute the correlation coefficient between the corresponding sampling views, \mathbf{v}_1 and \mathbf{v}_2 , as the intersection-over-union (IoU) ratio of the two sampled rectangles when they are put back to the original image plane. To avoid other factors that impact feature extraction, we only perform image cropping and rescaling during this testing procedure (*i.e.*, horizontal flipping and other color jittering operations are switched off).

Results are shown in Figure 2. The retrieval accuracy is closely related to the correlation between the sampled views. In other words, using strong data augmentation can deviate the objective of contrastive learning and thus harm the performance of downstream tasks. Intuitively, the difficulty comes from the inconsistency between the data sampling and contrastive learning stages in **dealing with spatial information**. Specifically, the sampling stage allows different views while the contrastive learning is built upon the encoding algorithm that mostly ignores spatial information.

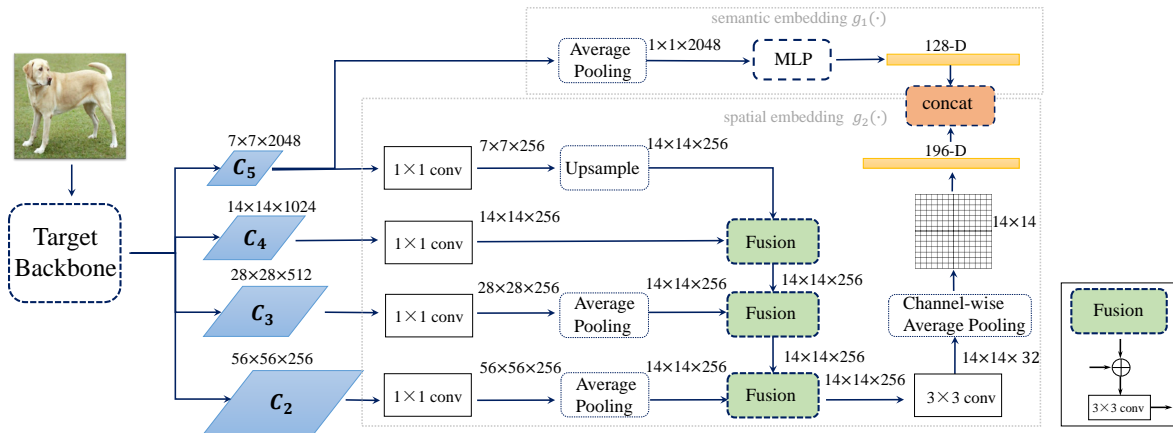


Figure 3. The framework of two-branch heterogeneous contrastive learning (HCL). The semantic branch is identical to the head of MoCo-v2 [3], and the spatial branch integrates multi-level features to capture spatial cues. The fusion module is illustrated in the right-hand side. The feature dimensionality is computed based on the ResNet series, yet HCL can be transplanted to other backbones.

3.3. Heterogeneous Contrastive Learning

To overcome the drawback, we explicitly encode spatial information into the embedding vector, $\mathbf{g}(\mathbf{x})$. The overall framework is shown in Figure 3. Different from the current approach that learns representations from a globally average-pooled feature vector (*i.e.*, with a spatial resolution of 1×1), we use an additional vector to capture spatial cues. This is to augment the concept of the embedding function from $\mathbf{g}(\cdot)$ to two individual branches, *i.e.*, $\mathbf{g}_1(\cdot)$ and $\mathbf{g}_2(\cdot)$. For simplicity and convenience of comparison, we assume that $\mathbf{g}_1(\cdot)$ is identical to $\mathbf{g}(\cdot)$ (*e.g.*, in training MoCo-v2 on ResNet-50, it is a two-layer perceptron upon the average-pooled feature from the C_5 layer), and $\mathbf{g}_2(\cdot)$ follows the design of feature pyramid network (FPN) [22] that combines information C_2 through C_5 . Similar to computing $\mathbf{g}_1(\cdot)$, there are learnable parameters for extracting $\mathbf{g}_2(\cdot)$ but these parameters will not be used for downstream tasks. Detailed configurations of $\mathbf{g}_1(\cdot)$ and $\mathbf{g}_2(\cdot)$, including the size of each layer, are illustrated in Figure 3. The outputs of $\mathbf{g}_1(\cdot)$ and $\mathbf{g}_2(\cdot)$ are separately normalized and then concatenated for contrastive learning. We name our approach **heterogeneous contrastive learning** (HCL), since $\mathbf{g}_1(\cdot)$ and $\mathbf{g}_2(\cdot)$ extract different sources of features (*i.e.*, $\mathbf{g}_1(\cdot)$ is mainly designed for semantics while $\mathbf{g}_2(\cdot)$ focuses on spatial information) for visual representation. Throughout the remainder of this paper, we refer to $\mathbf{g}_1(\cdot)$ and $\mathbf{g}_2(\cdot)$ as the semantic branch and spatial branch, respectively.

In our standard implementation, $\mathbf{g}_1(\cdot)$ and $\mathbf{g}_2(\cdot)$ produce 128-D and 196-D vectors, respectively, *i.e.*, the final representation vector has 324 dimensions, about $1.5 \times$ longer than the baseline (only using $\mathbf{g}_1(\cdot)$ to extract 128-D vectors). This brings two impacts. First, each unit (iteration or epoch) of contrastive learning is a little bit ($\sim 5.7\%$)

slower than the baseline, mainly caused by the additional cost in computing $\mathbf{g}_2(\cdot)$ and calculating Eqn (2) in a higher dimensionality. Second, the contrastive learning loss becomes lower (*i.e.*, the instance discrimination accuracy is higher), which is a direct benefit of using auxiliary spatial information for image representation. We will provide an essential explanation on this point in the next subsection. Nevertheless, note that all these changes happen in the contrastive learning procedure. Once it is finished, the pre-trained network can be deployed to any downstream tasks without additional overheads.

Before continuing to the next part, we try to answer an important question: why has HCL alleviated the inconsistency issue of representation learning? We owe this mainly to the contribution of the spatial branch. Assume that \mathbf{x}_1 and \mathbf{x}_2 are sampled using largely different views, \mathbf{v}_1 and \mathbf{v}_2 . The conventional contrastive learning algorithms, without the spatial branch, have to force the semantic embedding vectors to be very similar, *i.e.*, pulling $\mathbf{g}_1(\mathbf{x}_1)$ and $\mathbf{g}_1(\mathbf{x}_2)$ together. HCL, equipped with the spatial branch, has an extra opportunity of extracting close spatial embedding vectors. In the scenarios that \mathbf{v}_1 and \mathbf{v}_2 are weakly correlated (*e.g.*, the sampled images are partly overlapped), it is probable that the convolution and pooling operations in $\mathbf{g}_2(\cdot)$ can learn the correspondence between \mathbf{x}_1 and \mathbf{x}_2 and thus $\mathbf{g}_2(\mathbf{x}_1)$ and $\mathbf{g}_2(\mathbf{x}_2)$ are sufficiently close. Hence, the contrastive loss, Eqn (1), is optimized with a weaker constraint on the semantic embedding vectors. The above analysis also explains why the instance discrimination accuracy becomes higher (please refer to the next subsection for examples). However, it is still possible that sometimes, \mathbf{x}_1 and \mathbf{x}_2 (sampled from the same image) are totally non-overlapped. To solve this challenging case, we need a stronger function for

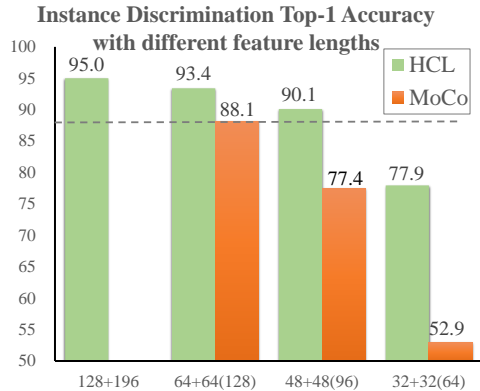


Figure 4. The instance discrimination accuracy with respect to different feature lengths, where HCL (mixed semantic and spatial embedding) enjoys significant advantages.

measuring image similarity, *e.g.*, going beyond calculating the inner-product of $\mathbf{g}(\mathbf{x}_1)$ and $\mathbf{g}(\mathbf{x}_2)$. We leave this study for future work.

3.4. Towards Efficient Visual Representations

This subsection aims to deliver an important message that HCL works better in capturing efficient visual representations. Intuitively, when each image is represented into a vector of fixed dimensionality, pursuing for a high instance discrimination accuracy is a proper task for S²VRL. In the contrastive learning framework, the dimensionality of the representation vector serves as a good criterion for the efficiency of representation, and hence we observe the accuracy of instance discrimination with the features of same dimensionality, encoded by different methods.

To ease the evaluation, we design an offline contrastive testing stage where the feature dimensionality can be freely adjusted. We perform a random shuffle on the ImageNet training set and maintain a queue of 65,536 images as the gallery. We perform principal component analysis (PCA) on the extracted features of these reference images and thus project the features to the spaces with the desired dimensionality. The projections for semantic and spatial features are individually computed. The whole training set is used for instance discrimination. Note that the network parameters are fixed, so although the gallery is updated after each iteration, no new learnable information is inserted. In this way, we can report the accuracy of instance discrimination with respect to different augmentation strengths and feature dimensionalities.

We test the standard augmentation strength as used in the training procedure, *i.e.*, a random cropping with image area lying in $[0.2, 1.0]$, random horizontal flipping, and random color jittering. We compare the representations learned from MoCo-v2 (trained on ImageNet-1K for 800 epochs)

and HCL model (trained on ImageNet-1K for 200 + 200 epochs – see Section 4.1 for details). We test the features under 64, 96, and 128 dimensions. In case of using HCL, each branch contributes half of feature dimensionality. The quantitative results are shown in Figure 4. HCL outperforms MoCo-v2 significantly in instance discrimination accuracy, especially under lower dimensionalities. This delivers the message that semantic and spatial representations are complementary, so combining them achieves higher instance discrimination accuracy. In the next part, we will show that HCL also achieves better performance in a wide range of downstream tasks.

3.5. Discussions and Relationship to Prior Work

Last but not least, we hope that our investigation inspires researchers in the community to focus on improving the efficiency of visual representations in S²VRL. Here, we leave some remarks for future research.

- **First**, we reveal that the current contrastive learning approach is suffering a conflict between strong data augmentation and accurate instance discrimination. Although introducing spatial information has improved the quality of visual representation, it is still difficult to cover the scenario when the spatial relationship between \mathbf{x}_1 and \mathbf{x}_2 is weak. To solve this problem under the contrastive learning framework, a better function for similarity computation (*i.e.*, $\text{sim}(\cdot, \cdot)$ in Eqn (1)) should be designed, equipped with the ability to predict that \mathbf{x}_1 and \mathbf{x}_2 are related even when they do not overlap at all.
- **Second**, we point out that instance discrimination accuracy is not a perfect standard for measuring the ability of preserving information. A clear counterexample lies in a learning-free algorithm that extracts a handful of local features (*e.g.*, SIFT [28]) from each image and uses them directly as visual representation. Since these features are robust to scale change, this algorithm may report high instance discrimination accuracy but it rarely helps S²VRL. We conjecture that a good learning objective should be somewhere between discrimination and generation (*i.e.*, recovering the original image with moderate details), the latter of which has been studied by some researchers [43, 34] but the progress seems to fall behind contrastive learning.

4. Experiments

4.1. Settings and Implementation Details

We use HCL to pre-train the backbone on the ImageNet-1K [5] dataset and then fine-tune the pre-trained model in downstream tasks. ImageNet-1K contains around 1.28M

Methods	Data	Mask R-CNN, R50-FPN, detection						Mask R-CNN, R50-FPN, instance segmentation					
		1× schedule			2× schedule			1× schedule			2× schedule		
		AP ^{bb}	AP ₅₀ ^{bb}	AP ₇₅ ^{bb}	AP ^{bb}	AP ₅₀ ^{bb}	AP ₇₅ ^{bb}	AP ^{bb}	AP ₅₀ ^{bb}	AP ₇₅ ^{bb}	AP ^{bb}	AP ₅₀ ^{bb}	AP ₇₅ ^{bb}
Supervised	IN	38.9	59.6	42.7	40.6	61.3	44.4	35.4	56.5	38.1	36.8	58.1	39.5
MoCo-v1	IN	38.5	58.9	42.0	40.8	61.6	44.7	35.1	55.9	37.7	36.9	58.4	39.7
MoCo-v2	IN	39.2	59.9	42.7	41.6	62.1	45.6	35.7	56.8	38.1	37.7	59.3	40.6
MoCo-v1	IG	38.9	59.4	42.3	41.1	61.8	45.1	35.4	56.5	37.9	37.4	59.1	40.2
HCL	IN	40.0	60.6	43.8	41.8	62.4	45.7	36.4	57.6	39.1	37.8	59.5	40.8

Table 1. Object detection and instance segmentation fine-tuned Mask R-CNN with the R50-FPN backbone on MS-COCO (averaged by 3 runs). IN in tables means model pre-trained on ImageNet-1K [5] dataset (1M images) and IG represents Instagram dataset [25] (1B images).

Methods	Data	Mask R-CNN, R50-C4, detection						Mask R-CNN, R50-C4, instance segmentation					
		1× schedule			2× schedule			1× schedule			2× schedule		
		AP ^{bb}	AP ₅₀ ^{bb}	AP ₇₅ ^{bb}	AP ^{bb}	AP ₅₀ ^{bb}	AP ₇₅ ^{bb}	AP ^{bb}	AP ₅₀ ^{bb}	AP ₇₅ ^{bb}	AP ^{bb}	AP ₅₀ ^{bb}	AP ₇₅ ^{bb}
Supervised	IN	38.2	58.2	41.2	40.0	59.9	43.1	33.3	54.7	35.2	34.7	56.5	36.9
MoCo-v1	IN	38.5	58.3	41.6	40.7	60.5	44.1	33.6	54.8	35.6	35.4	57.3	37.6
MoCo-v2	IN	39.5	59.1	42.7	41.2	61.0	44.8	34.5	55.8	36.7	35.8	57.6	38.3
MoCo-v1	IG	39.1	58.7	42.2	41.1	60.7	44.8	34.1	55.4	36.4	35.6	57.4	38.1
HCL	IN	39.8	59.3	43.3	41.4	61.1	45.0	34.7	56.2	37.0	35.9	57.9	38.3

Table 2. Object detection and instance segmentation fine-tuned Mask R-CNN with the R50-C4 backbone on COCO (averaged by 3 runs).

training images in 1,000 classes. The validation set containing 50K images is not used. We do not use the semantic labels during the pre-training stage, and merely rely on the instance discrimination task to extract powerful features that are transferrable to the downstream tasks.

Following the setting of MoCo-v2 [3], we choose the ResNet-50 [15] as the backbone and configure a memory bank with a size of 65,536. There are two stages in training the HCL model. The first stage, known as the warm-up process, is identical to MoCo-v2 and lasts 200 epochs. After that, the second stage trains the full HCL model for another 200 epochs. In the second stage, we adjust the initial learning rate to 0.05 with the cosine annealing schedule and adopt the SGD optimizer with a momentum of 0.9. The mini-batch size is 256 in both stages. The two-stage design is to make sure that the network has a basic ability in capturing semantic features – without it, the training procedure often suffers turbulence. The numbers of epochs in both stages are important hyper-parameters for HCL, which we will diagnose in the later experiments. Under the standard 200-epoch setting, the two training stages take around 50 and 53 hours on eight NVIDIA Tesla-V100 GPUs, respectively.

Note that both stages of pre-training need to be performed only once and can be deployed to a series of downstream tasks just like the models trained with full supervisions. Although HCL introduces a FPN-like architecture to capture the spatial information, the pre-trained weights on these layers are not inherited by the downstream tasks. This is to make a fair comparison to other pre-trained models, in

particular, MoCo-v2.

4.2. Performance in Downstream Tasks

We evaluate our approach for object detection and semantic/instance segmentation, and compare the performance to supervised pre-training and MoCo-v1/v2. The used datasets include MS-COCO [23], LVIS [12], Pascal VOC [8], and Cityscapes [4]. For a fair comparison, all settings in the downstream tasks are same as that in MoCo-v1/v2.

4.2.1 MS-COCO: Detection and Segmentation

We first evaluate HCL on MS-COCO, a popular benchmark for object detection and instance segmentation. We use the Mask R-CNN [14] framework that accomplishes detection and segmentation simultaneously, and equip it with the pre-trained ResNet-50 backbone and either the FPN or C4 heads. All the network layers are fine-tuned on the COCO2017 training set, and we follow the convention to report the average precision (AP) on the validation set under different learning schedules (known as 1× and 2×).

The results using FPN and C4 heads are summarized in Table 1 and Table 2, respectively. One can observe that HCL surpasses the competitors consistently. The gains are more significant under the 1× setting, where the FPN-equipped HCL outperforms the corresponding MoCo-v2 by 0.8% and 0.7% in terms of detection and segmentation APs, respectively. Besides, HCL also surpasses the supervised pre-training backbone and the MoCo-v1 model using 1 bil-

Methods	Data	BN	AP ^{bb}	AP ₅₀ ^{bb}	AP ₇₅ ^{bb}
Supervised	IN	frozen	24.4	37.5	25.8
Supervised	IN	tuned	23.2	36.0	24.4
MoCo-v1	IN	tuned	24.1	37.4	25.5
MoCo-v2	IN	tuned	25.3	38.4	27.0
MoCo-v1	IG	tuned	24.9	38.2	26.4
HCL	IN	tuned	25.5	38.9	27.2

Table 3. Long-tailed instance segmentation fine-tuned Mask R-CNN with the R50-FPN backbone and $2\times$ schedule on LVIS-v05 (averaged by 3 runs).

lion unlabeled images, demonstrating its higher efficiency in learning visual representations.

It is also interesting to see that under the $1\times$ setting, the advantage of MoCo-v2 over supervised training is not as big as HCL enjoys, which delivers the message that the model converges faster when it is initialized by HCL. We conjecture that such benefits imply the nature that object detection and instance segmentation require the model to have stronger abilities in extracting spatial cues. Therefore, by explicitly encoding spatial information during the pre-training stage, HCL is easily adjusted to these downstream tasks, and has a higher upper-bound though the advantages can shrink as the schedule becomes longer.

4.2.2 LVIS: Instance Segmentation

Next, we evaluate HCL on the LVIS-v0.5 dataset for instance segmentation. Different from MS-COCO in which images fall into common categories with abundant labels, LVIS is closer to the real-world recognition scenario that the objects form a long-tail distribution. Therefore, a good practice in LVIS provides more evidences on transferability of the pre-trained backbone. We follow the convention to use the Mask R-CNN model with FPN, and perform the fine-tuning process with a $2\times$ schedule.

The segmentation results on the validation set are shown in Table 3. HCL produces comparable results to MoCo-v2, and outperforms the supervised backbone once again. These results once again imply that spatial information is complementary to semantic information, and HCL boosts the potential of the pre-trained backbone.

4.2.3 PASCAL VOC: Detection and Segmentation

We then test the tasks of object detection and semantic segmentation on the PASCAL VOC dataset. For the detection task, we use the Detectron2 library [42] to fine-tune Faster R-CNN [35] with a ResNet-50 backbone and a C4 head. Follow the settings of MoCo, the fine-tuning lasts for 24K iterations (the $2\times$ schedule) on the *trainval* set of VOC₀₇₊₁₂, and the testing is done on the *test* set of VOC₀₇. All the training images are rescaled so that the

Methods	Data	detection			seg
		AP ^{bb}	AP ₅₀ ^{bb}	AP ₇₅ ^{bb}	mIoU
Supervised	IN	53.5	81.4	58.8	74.4
MoCo-v1	IN	55.9	81.5	62.6	72.5
MoCo-v2	IN	57.4	82.5	64.0	73.4
MoCo-v1	IG	57.2	82.5	63.7	73.6
HCL	IN	57.9	82.7	64.9	74.1

Table 4. Object detection and semantic segmentation results on PASCAL VOC dataset after fine-tuning (averaged by 3 runs).

Methods	Data	instance seg		semantic seg
		AP ^{bb}	AP ₅₀ ^{bb}	mIoU
Supervised	IN	32.9	59.6	74.6
MoCo-v1	IN	32.3	59.3	75.3
MoCo-v2	IN	33.1	60.1	75.1
MoCo-v1	IG	32.9	60.3	75.5
HCL	IN	33.1	60.2	75.2
HCL*	IN	33.6	60.8	75.5

Table 5. Segmentation results on the Cityscapes dataset (averaged by 3 runs). * indicates that the HCL model is trained for 800 epochs in the first stage.

shorter edge length falls in $[400, 800]$, and the testing images are in the original size. For the segmentation task, we fine-tune FCN [24] with the ResNet-50 backbone for 50K iterations, use the *train* set of VOC₁₂ for training and the *val* set of VOC₁₂ for testing.

Results are summarized in Table 4. For the detection task, HCL outperforms both MoCo and the supervised backbone, especially in terms of the AP₇₅^{bb} metric where the advantages over the supervised and MoCo counterparts are 6.1% and 0.9%, respectively. This phenomenon aligns with that in MS-COCO experiments. Since AP₇₅^{bb} has a higher requirement in localization, we confirm that extracting spatial information in the pre-training stage is helpful to localization. For the segmentation task, HCL surpasses MoCo-v2 by a gain of 0.7%, largely shrinking the deficit to the supervised baseline. HCL is the best in terms of the overall detection and segmentation performance.

4.2.4 Cityscapes: Instance/Semantic Segmentation

As the last downstream task, we evaluate the Cityscapes dataset for instance and semantic segmentation in the natural scene images. We use the Mask R-CNN model with FPN as the head and use the $2\times$ schedule. The results of different pre-trained models are summarized in Table 5. To alleviate randomness, we repeat the fine-tuning process three times and report the averaged numbers.

The best pre-trained models in this scenario are HCL and the MoCo-v1 model pre-trained on 1 billion images. This is as expected, since the domain of Cityscapes is largely different from that of ImageNet (auto-driving scenarios, high-

resolution), so that the backbone may suffer a domain gap if it is pre-trained **only** in ImageNet-1K and the spatial information is ignored. MoCo-v1 gains stronger transferability by accessing much more unlabeled image data, yet HCL achieves comparable and even better performance by learning more efficient visual representations, where the latter can save considerable costs in data annotation.

Interestingly, with a longer pre-training stage (the first stage is extended from 200 to 800 epochs), the accuracy of HCL continues going up yet MoCo-v2 has arrived at a plateau (with 1,000 epochs, the gain over using 800 epochs is less than 0.1%). We refer the readers to the next section in which we will discuss how the pre-training schedule affects the recognition performance.

4.3. Diagnostic Studies

4.3.1 Different Training Schedules

HCL has two pre-training stages, and different training schedules of these stages can affect the recognition performance. Table 6 summarizes some comparative results using different numbers of pre-training epochs. From the detection results on the MS-COCO dataset, one can observe that both stages contribute to the recognition accuracy. In particular, (i) skipping the first stage causes a 0.5% drop in both detection and segmentation APs; (ii) undergoing 200 or 800 epochs in the first stage does not bring a big difference especially when the second stage is present; and (iii) extending the second stage from 200 to 400 epochs leads to consistent accuracy drop.

Integrating the above results yields a big picture of heterogeneous contrastive learning that semantic feature learning serves as a good basis for spatial feature learning, but these two features still seem to conflict because of the different learning goals. Currently, the best choice is to assign 200 epochs to each stage, so that with a total of 400 epochs, the pre-trained model surpasses the MoCo-v2 model with 800 epochs while the computational costs are shrunk by half. Nevertheless, alleviating the conflict and allowing a longer training schedule is important for future research.

4.3.2 Design of the Spatial Branch

The design of the spatial branch mostly follows the FPN module that integrates four layers of ResNet-50 into the final features. Note that we desire a 14×14 map in the end (so that 196 is comparable to 128). Unlike the vanilla FPN that integrates all features into a spatial resolution of 56×56 (and then down-samples it into 14×14), we slightly modify the architecture so that two average-pooling layers are inserted into the third and fourth paths so that the output is directly in 14×14 . This modification does not affect the recognition accuracy (*e.g.*, on MS-COCO with FPN, the detection and segmentation APs using the vanilla FPN is

Mask R-CNN, R50-FPN, $1 \times$ schedule			
Stage 1	Stage 2	COCO _{Det}	COCO _{Seg}
200	0	38.9	35.4
800	0	39.2	35.7
0	200	39.5	35.9
200	200	40.0	36.4
800	200	40.1	36.2
200	400	39.7	36.1
800	400	39.6	36.0

Table 6. The results of pre-trained models with different training epochs in the first and second stages on MS-COCO (averaged by 3 runs). The numbers in the top two lines are achieved by MoCo models.

39.9% and 36.1%, respectively, comparable to our results, 40.0% and 36.4%), but thanks to the reduced spatial resolution, our design saves around 10% training cost in the second pre-training stage.

Another important issue is whether to inherit the pre-trained weights in FPN to the downstream tasks, if available. In practice, either option produces similar performance in the downstream tasks, indicating that the initialization of the FPN weights seems less important. For a fair comparison, we switch off this option in the main experiments.

4.3.3 The Effect of Horizontal Flipping

In the original contrastive learning baseline, horizontal flipping is a standard operation that forces the backbone to output similar features for an image and its reversed copy. However, when the spatial branch is present, horizontal flipping can cause a mismatch between the spatial features. Not surprisingly, switching off the option of flipping improves the downstream performance (*e.g.*, on MS-COCO with FPN, the detection and segmentation APs with flipping are 39.6% and 36.0%, respectively, both are 0.4% lower than that without flipping). The AP of instance segmentation in LVIS-v0.5 also drops by 0.5% with the flipping augmentation switched on. This inspires us that HCL has changed the requirement of data augmentation, and implies the difficulty of integrating semantic and spatial cues into the pre-trained models.

5. Conclusions

This paper reveals an important problem that spatial information is ignored in the contrastive learning frameworks, so that strong data augmentation including image cropping and flipping can confuse the algorithms, causing a conflict between instance discrimination and representation learning. To alleviate the problem, we propose heterogeneous contrastive learning (HCL) that inserts a branch to capture

spatial information and concatenate the semantic and spatial features for contrastive learning. Experiments show that HCL not only achieves better performance in a series of downstream tasks, but also enjoys a higher efficiency in visual representations. We argue that these two factors are closely related, and thus advocate for further study along this direction to improve S²VRL. In the future, we will also integrate supervised learning into our algorithm [41].

References

- [1] Anonymous. Contrastive learning with stronger augmentations. https://openreview.net/forum?id=KJSC_AsN14, 2010. 1, 3
- [2] Ting Chen, Simon Kornblith, Mohammad Norouzi, and Geoffrey Hinton. A simple framework for contrastive learning of visual representations. *arXiv preprint arXiv:2002.05709*, 2020. 1, 2, 3
- [3] Xinlei Chen, Haoqi Fan, Ross Girshick, and Kaiming He. Improved baselines with momentum contrastive learning. *arXiv preprint arXiv:2003.04297*, 2020. 1, 2, 3, 4, 6
- [4] Marius Cordts, Mohamed Omran, Sebastian Ramos, Timo Rehfeld, Markus Enzweiler, Rodrigo Benenson, Uwe Franke, Stefan Roth, and Bernt Schiele. The cityscapes dataset for semantic urban scene understanding. In *Proceedings of the IEEE conference on computer vision and pattern recognition*, pages 3213–3223, 2016. 6
- [5] Jia Deng, Wei Dong, Richard Socher, Li-Jia Li, Kai Li, and Li Fei-Fei. Imagenet: A large-scale hierarchical image database. In *2009 IEEE conference on computer vision and pattern recognition*, pages 248–255. Ieee, 2009. 2, 5, 6
- [6] Carl Doersch, Abhinav Gupta, and Alexei A Efros. Unsupervised visual representation learning by context prediction. In *Proceedings of the IEEE international conference on computer vision*, pages 1422–1430, 2015. 1, 2
- [7] Alexey Dosovitskiy, Jost Tobias Springenberg, Martin Riedmiller, and Thomas Brox. Discriminative unsupervised feature learning with convolutional neural networks. In *Advances in neural information processing systems*, pages 766–774, 2014. 1
- [8] Mark Everingham, Luc Van Gool, Christopher KI Williams, John Winn, and Andrew Zisserman. The pascal visual object classes (voc) challenge. *International journal of computer vision*, 88(2):303–338, 2010. 6
- [9] Basura Fernando, Hakan Bilen, Efstratios Gavves, and Stephen Gould. Self-supervised video representation learning with odd-one-out networks. In *Proceedings of the IEEE conference on computer vision and pattern recognition*, pages 3636–3645, 2017. 2
- [10] Spyros Gidaris, Praveer Singh, and Nikos Komodakis. Unsupervised representation learning by predicting image rotations. *arXiv preprint arXiv:1803.07728*, 2018. 1, 2
- [11] Jean-Bastien Grill, Florian Strub, Florent Altché, Corentin Tallec, Pierre H Richemond, Elena Buchatskaya, Carl Doersch, Bernardo Avila Pires, Zhaohan Daniel Guo, Mohammad Gheshlaghi Azar, et al. Bootstrap your own latent: A new approach to self-supervised learning. *arXiv preprint arXiv:2006.07733*, 2020. 1
- [12] Agrim Gupta, Piotr Dollar, and Ross Girshick. Lvis: A dataset for large vocabulary instance segmentation. In *Proceedings of the IEEE Conference on Computer Vision and Pattern Recognition*, pages 5356–5364, 2019. 6
- [13] Kaiming He, Haoqi Fan, Yuxin Wu, Saining Xie, and Ross Girshick. Momentum contrast for unsupervised visual representation learning. In *Proceedings of the IEEE/CVF Conference on Computer Vision and Pattern Recognition*, pages 9729–9738, 2020. 1, 2, 3
- [14] Kaiming He, Georgia Gkioxari, Piotr Dollár, and Ross Girshick. Mask r-cnn. In *Proceedings of the IEEE international conference on computer vision*, pages 2961–2969, 2017. 6
- [15] Kaiming He, Xiangyu Zhang, Shaoqing Ren, and Jian Sun. Deep residual learning for image recognition. In *Proceedings of the IEEE conference on computer vision and pattern recognition*, pages 770–778, 2016. 6
- [16] Po-Han Huang, Kevin Matzen, Johannes Kopf, Narendra Ahuja, and Jia-Bin Huang. Deepmvs: Learning multi-view stereopsis. In *Proceedings of the IEEE Conference on Computer Vision and Pattern Recognition*, pages 2821–2830, 2018. 2
- [17] Prannay Khosla, Piotr Teterwak, Chen Wang, Aaron Sarna, Yonglong Tian, Phillip Isola, Aaron Maschinot, Ce Liu, and Dilip Krishnan. Supervised contrastive learning. *arXiv preprint arXiv:2004.11362*, 2020. 1, 3
- [18] Gustav Larsson, Michael Maire, and Gregory Shakhnarovich. Colorization as a proxy task for visual understanding. In *Proceedings of the IEEE Conference on Computer Vision and Pattern Recognition*, pages 6874–6883, 2017. 2
- [19] Yann LeCun, Yoshua Bengio, and Geoffrey Hinton. Deep learning. *nature*, 521(7553):436–444, 2015. 1, 2
- [20] Hsin-Ying Lee, Jia-Bin Huang, Maneesh Singh, and Ming-Hsuan Yang. Unsupervised representation learning by sorting sequences. In *Proceedings of the IEEE International Conference on Computer Vision*, pages 667–676, 2017. 2
- [21] Hao Li, Xiaopeng Zhang, Ruoyu Sun, Hongkai Xiong, and Qi Tian. Center-wise local image mixture for contrastive representation learning. *arXiv preprint arXiv:2011.02697*, 2020. 1, 3
- [22] Tsung-Yi Lin, Piotr Dollár, Ross Girshick, Kaiming He, Bharath Hariharan, and Serge Belongie. Feature pyramid networks for object detection. In *Proceedings of the IEEE conference on computer vision and pattern recognition*, pages 2117–2125, 2017. 2, 4
- [23] Tsung-Yi Lin, Michael Maire, Serge Belongie, James Hays, Pietro Perona, Deva Ramanan, Piotr Dollár, and C Lawrence Zitnick. Microsoft coco: Common objects in context. In *European conference on computer vision*, pages 740–755. Springer, 2014. 2, 6
- [24] Jonathan Long, Evan Shelhamer, and Trevor Darrell. Fully convolutional networks for semantic segmentation. In *Proceedings of the IEEE conference on computer vision and pattern recognition*, pages 3431–3440, 2015. 7
- [25] Dhruv Mahajan, Ross Girshick, Vignesh Ramanathan, Kaiming He, Manohar Paluri, Yixuan Li, Ashwin Bharambe, and Laurens van der Maaten. Exploring the limits of weakly

- supervised pretraining. In *Proceedings of the European Conference on Computer Vision (ECCV)*, pages 181–196, 2018. [6](#)
- [26] Tomasz Malisiewicz and Alyosha Efros. Beyond categories: The visual memex model for reasoning about object relationships. In *Advances in neural information processing systems*, pages 1222–1230, 2009. [2](#)
- [27] Ishan Misra, C Lawrence Zitnick, and Martial Hebert. Shuffle and learn: unsupervised learning using temporal order verification. In *European Conference on Computer Vision*, pages 527–544. Springer, 2016. [2](#)
- [28] Pauline C Ng and Steven Henikoff. Sift: Predicting amino acid changes that affect protein function. *Nucleic acids research*, 31(13):3812–3814, 2003. [5](#)
- [29] Mehdi Noroozi and Paolo Favaro. Unsupervised learning of visual representations by solving jigsaw puzzles. In *European Conference on Computer Vision*, pages 69–84. Springer, 2016. [1](#), [2](#)
- [30] Mehdi Noroozi, Hamed Pirsiavash, and Paolo Favaro. Representation learning by learning to count. In *Proceedings of the IEEE International Conference on Computer Vision*, pages 5898–5906, 2017. [2](#)
- [31] Mehdi Noroozi, Ananth Vinjimoor, Paolo Favaro, and Hamed Pirsiavash. Boosting self-supervised learning via knowledge transfer. In *Proceedings of the IEEE Conference on Computer Vision and Pattern Recognition*, pages 9359–9367, 2018. [2](#)
- [32] Deepak Pathak, Ross Girshick, Piotr Dollár, Trevor Darrell, and Bharath Hariharan. Learning features by watching objects move. In *Proceedings of the IEEE Conference on Computer Vision and Pattern Recognition*, pages 2701–2710, 2017. [2](#)
- [33] Deepak Pathak, Philipp Krahenbuhl, Jeff Donahue, Trevor Darrell, and Alexei A Efros. Context encoders: Feature learning by inpainting. In *Proceedings of the IEEE conference on computer vision and pattern recognition*, pages 2536–2544, 2016. [2](#)
- [34] Guo-Jun Qi, Liheng Zhang, Chang Wen Chen, and Qi Tian. Avt: Unsupervised learning of transformation equivariant representations by autoencoding variational transformations. In *Proceedings of the IEEE International Conference on Computer Vision*, 2019. [5](#)
- [35] Shaoqing Ren, Kaiming He, Ross Girshick, and Jian Sun. Faster r-cnn: Towards real-time object detection with region proposal networks. In *Advances in neural information processing systems*, pages 91–99, 2015. [7](#)
- [36] Rodrigo Santa Cruz, Basura Fernando, Anoop Cherian, and Stephen Gould. Deeppermnet: Visual permutation learning. In *Proceedings of the IEEE Conference on Computer Vision and Pattern Recognition*, pages 3949–3957, 2017. [2](#)
- [37] Yonglong Tian, Chen Sun, Ben Poole, Dilip Krishnan, Cordelia Schmid, and Phillip Isola. What makes for good views for contrastive learning. *arXiv preprint arXiv:2005.10243*, 2020. [2](#)
- [38] Weiran Wang, Raman Arora, Karen Livescu, and Jeff Bilmes. On deep multi-view representation learning. In *International conference on machine learning*, pages 1083–1092, 2015. [2](#)
- [39] Xiaolong Wang and Abhinav Gupta. Unsupervised learning of visual representations using videos. In *Proceedings of the IEEE international conference on computer vision*, pages 2794–2802, 2015. [2](#)
- [40] Chen Wei, Lingxi Xie, Xutong Ren, Yingda Xia, Chi Su, Jiaying Liu, Qi Tian, and Alan L Yuille. Iterative reorganization with weak spatial constraints: Solving arbitrary jigsaw puzzles for unsupervised representation learning. In *Proceedings of the IEEE Conference on Computer Vision and Pattern Recognition*, pages 1910–1919, 2019. [2](#)
- [41] Longhui Wei, Lingxi Xie, Jianzhong He, Jianlong Chang, Xiaopeng Zhang, Wengang Zhou, Houqiang Li, and Qi Tian. Can semantic labels assist self-supervised visual representation learning? *arXiv preprint arXiv:2011.08621*, 2020. [9](#)
- [42] Yuxin Wu, Alexander Kirillov, Francisco Massa, Wan-Yen Lo, and Ross Girshick. Detectron2, 2019. [7](#)
- [43] Liheng Zhang, Guo-Jun Qi, Liqiang Wang, and Jiebo Luo. Aet vs. aed: Unsupervised representation learning by autoencoding transformations rather than data. In *Proceedings of the IEEE Conference on Computer Vision and Pattern Recognition*, 2019. [5](#)
- [44] Richard Zhang, Phillip Isola, and Alexei A Efros. Colorful image colorization. In *European conference on computer vision*, pages 649–666. Springer, 2016. [2](#)